

# $^{18}\text{F}$ -FDG PET Detection of Lymph Node Metastases in Medullary Thyroid Carcinoma

Szabolcs Szakáll, Jr., MD<sup>1</sup>; Olga Ésik, DSc<sup>2,3</sup>; Gábor Bajzik, PhD<sup>4</sup>; Imre Repa, PhD<sup>4</sup>; Gabriella Dabasi, PhD<sup>5</sup>; István Sinkovics, PhD<sup>6</sup>; Péter Ágoston, MD<sup>2</sup>; and Lajos Trón, DSc<sup>1</sup>

<sup>1</sup>PET Center, University of Debrecen, Debrecen, Hungary; <sup>2</sup>Department of Radiotherapy, National Institute of Oncology, Budapest, Hungary; <sup>3</sup>Department of Radiotherapy, Semmelweis University, Budapest, Hungary; <sup>4</sup>Diagnostic Center, University of Kaposvár, Kaposvár, Hungary; <sup>5</sup>Department of Surgery and Transplantation, Semmelweis University, Budapest, Hungary; and <sup>6</sup>Department of Nuclear Medicine, National Institute of Oncology, Budapest, Hungary

Postsurgically elevated or increasing serum calcitonin levels strongly suggest the presence of residual or recurrent medullary thyroid carcinoma (MTC). Several imaging modalities (sonography, MRI, CT, scintigraphy with different types of radiolabeled ligands, etc.) are routinely used in an attempt to localize tumorous tissue, but such efforts often fail. In the search for a more reliable method,  $^{18}\text{F}$ -FDG PET was applied to detect tumor tissue of residual or recurrent MTC. **Methods:** Forty patients with a postoperatively elevated plasma calcitonin level were included. These patients underwent routine diagnostic imaging procedures (CT, MRI, and  $^{131}\text{I}$ -metaiodobenzylguanidine [MIBG] whole-body planar scintigraphy or SPECT) and  $^{18}\text{F}$ -FDG PET examinations. Two independent experts visually analyzed the images provided by each method to detect pathologic lesions. Lymph nodes of  $\geq 1$  cm in short diameter that were detected by radiologic methods were considered to be pathologic.  $^{18}\text{F}$ -FDG accumulation with a sharp contour reported by both independent observers was similarly regarded as pathologic. **Results:** PET detected 270 foci with a high tracer accumulation, whereas only 116 lesions were detected by MRI and 141 by CT. The numbers of such foci determined by PET, MRI, and CT were 98, 34, and 34, respectively, in the neck; 25, 5, and 6, respectively, in the supraclavicular regions; and 117, 35, and 39, respectively, in the mediastinum.  $^{131}\text{I}$ -MIBG scintigraphy findings were positive for only 3 patients. **Conclusion:** For MTC patients with a postoperatively elevated plasma tumor marker level, PET was more sensitive and superior in localizing tumorous lymph node involvement than were the other imaging modalities, especially in the cervical, supraclavicular, and mediastinal lymphatic regions.

**Key Words:** PET;  $^{18}\text{F}$ -FDG; medullary thyroid cancer; lymph node metastasis

**J Nucl Med 2002; 43:66–71**

**M**edullary thyroid carcinoma (MTC) originating from the calcitonin-secreting parafollicular cells (C cells) is a relatively rare disease, composing 3%–10% of all malignant

thyroid tumors (1). The familial forms, which account for 25% of all MTCs, include 3 well-defined syndromes: familial MTC and multiple endocrine neoplasia types 2A and 2B. The remainder (75%) of MTCs are sporadic. Among the metastases, lymph node involvement is the most common throughout the clinical course. During initial staging, the incidence of pathologically proven cervical lymph node metastases has been reported to be 71%–80% (2–4); the corresponding value for mediastinal involvement is 36% (2,4), whereas distant metastases have been reported in 20% of MTC patients (5).

Postsurgically elevated basal serum calcitonin and carcinoembryonic antigen (CEA) levels suggest persisting tumorous tissue (6), and testing of the levels of these plasma markers is therefore the most frequently applied method in long-term follow-up. Selective venous catheterization (7,8), with a correct localization rate of 89%, is the gold standard for identification of residual or recurrent lymph nodes; however, its invasiveness restricts its general use. Morphologic imaging methods can confirm the involvement of lymph nodes on the basis of their size, but these investigations are often insufficient because of the smallness of the tumorous lesions (9,10). Sonography has shown a lymph node detection rate of 28%–78% (11,12), compared with 38%–70% for CT (11,12) and 44%–74% for MRI (13,14). Various tumor-avid radiotracers, such as  $^{201}\text{Tl}$ -chloride,  $^{123}\text{I}$ - or  $^{131}\text{I}$ -metaiodobenzylguanidine (MIBG), radiolabeled anti-CEA antibodies, pentavalent  $^{99\text{m}}\text{Tc}$ -dimercaptosuccinic acid, and  $^{111}\text{In}$ -pentetreotide, have been used for tumor imaging with limited efficacy (15–22).

The accumulation of  $^{18}\text{F}$ -FDG in malignant tissue is well known; it is influenced by the grade of malignancy, related to glycolysis (23).  $^{18}\text{F}$ -FDG has been successfully used in the follow-up of patients with differentiated thyroid cancer (24–30). There are similar reports on  $^{18}\text{F}$ -FDG PET investigations in MTC; however, the number of patients involved in these studies was generally  $<10$  (31–34), with the exception of a single study (35) in which 20 patients were investigated.

We report data on the application of  $^{18}\text{F}$ -FDG PET in several MTC cases and compare the results of this method

Received Feb. 16, 2001; revision accepted Aug. 20, 2001.

For correspondence or reprints contact: Szabolcs Szakáll, MD, PET Center, University of Debrecen, Nagyerdei körút 98, H-4012 Debrecen, Hungary.  
E-mail: [szakall@pet.dote.hu](mailto:szakall@pet.dote.hu)

with those of conventional imaging procedures for the diagnosis of residual or recurrent MTC.

## MATERIALS AND METHODS

### Patients

Forty nondiabetic patients (18 men, 22 women; age range, 23–69 y; mean age  $\pm$  SD,  $48 \pm 11$  y) with a history of MTC (15 hereditary, 19 sporadic, and 6 undetermined) were included in this investigation. The initial histologic result, including the immunophenotyping of each case, was revised by an independent pathologist. All but 1 patient had undergone total, near-total, or subtotal thyroidectomy, and 28 had undergone lymph node dissection, node picking, or both. The only exception was a patient who had a sternotomy because of the atypical localization of the primary tumor in the mediastinum.

External irradiation was used as supplementary therapy in 30 patients, 7 received  $^{131}\text{I}$ -MIBG radionuclide therapy, and 3 had chemotherapy. As tumor markers, the basal plasma calcitonin level (reference level,  $<10$  ng/mL) was measured by human calcitonin enzyme-linked immunosorbent assay (CIS Bio International, Gif sur Yvette, France) with 2 monoclonal antibodies, and CEA (reference level,  $<6$  ng/mL) was determined by luminometry. The marker levels were assessed postsurgically after 2 mo and at 6-mo intervals thereafter. Details of the individual patients are displayed in Table 1.

### Imaging

All diagnostic imaging examinations of the same patient were performed at least 2 mo after any therapy and were completed within a 3-mo interval. Written consent was obtained from all patients before the start of the procedures.  $^{18}\text{F}$ -FDG PET studies were performed with a 4096 Plus scanner (General Electric, Uppsala, Sweden) providing fifteen 2-dimensional sections over an axial field of view of 10 cm. The in-plane resolution was 5.5 mm (full width at half maximum), and the axial resolution was 6 mm. To suppress myocardial uptake, patients had to fast for at least 4 h before receiving 5.55 MBq/kg (0.15 mCi/kg)  $^{18}\text{F}$ -FDG by intravenous injection. The patients were also requested to abstain from physical activity before injection and until scanning. Whole-body examinations were begun from the base of the pelvis 40 min after the administration of  $^{18}\text{F}$ -FDG (7–9 bed positions, 10 min acquisition time per position). The acquired data were reconstructed using filtered backprojection with a Hanning filter (cutoff,  $0.5 \text{ pixels}^{-1}$ ). To avoid the extra inconvenience to the patients of a lengthy transmission scan, which would have been required because of the lack of an iterative reconstruction and segmentation algorithm in the software bundled with the camera, we did not correct for tissue attenuation.

Native and contrast-enhanced helical CT scanning was performed with a Somatom HR (Siemens, Erlangen, Germany) scanner, with a slice thickness of 5 mm from the base of the skull to the apex of the lung and a slice thickness of 10 mm for the rest of the body. Axial and coronal unenhanced T1-, T2-, and proton-weighted images of the neck, chest, and abdomen were obtained with a 1.5-T MRI unit (Magnetom; Siemens) for all patients, excluding 5 individuals with claustrophobia. The T1 axial sequences were repeated after the administration of contrast material.

Overlapping multiple planar images of the whole body were obtained for all patients with a Starcam 600XR/T (General Electric Medical Systems, Milwaukee, WI) or GCA-7100DI (Toshiba

Corp., Tokyo, Japan) gamma camera, 48–72 h after the injection of 40 MBq  $^{131}\text{I}$ -MIBG. Additional SPECT scans of the neck and thorax were obtained for some patients with a high-energy parallel-hole collimator.

### Interpretation

The number of pathologic foci was determined by visual assessment of the reconstructed images of the individual imaging modalities by 2 experts.  $^{18}\text{F}$ -FDG accumulation with a sharp contour reported by both independent observers was regarded as pathologic. Lymph nodes of  $\geq 1$  cm in short diameter that were detected by radiologic methods were likewise considered to be pathologic.

## RESULTS

Elevated calcitonin levels (range, 14.5–5,827 ng/mL; mean  $\pm$  SD,  $1,246.44 \pm 1,505.43$  ng/mL) were detected in all 40 patients, 25 of whom had a CEA level (range, 6.5–694.5 ng/mL; mean  $\pm$  SD,  $120.13 \pm 176.02$  ng/mL) above the reference range.

Various numbers of involved lymph nodes and other metastases were visualized through the different imaging modalities for all patients studied (Tables 2 and 3). PET scans were conclusive for 38 patients, showing 98 cervical, 25 supraclavicular, 4 axillary, 117 mediastinal, 3 abdominal, 14 hepatic, 6 osseous, and 2 pulmonary lesions with a high  $^{18}\text{F}$ -FDG uptake, whereas CT revealed 34, 6, 3, 39, 3, 24, 0, and 31 such lesions, respectively, and MRI revealed 34, 5, 1, 35, 0, 16, 2, and 22, respectively. In addition, a breast metastasis was found in 1 patient; it was detected by CT, MRI, and PET (Fig. 1) and was confirmed by histology. Thyroid remnants were confirmed by CT, MRI, sonography, or thyroid scintigraphy for patients having a less radical thyroidectomy (near-total or subtotal). In these patients (8/31, 26%), a total of 12 lesions with  $^{18}\text{F}$ -FDG uptake were present in the central cervical region at the site of the thyroid bed. These accumulations associated with the physiologic uptake by the thyroid remnants were not included in the number of lesions found by PET. When PET was compared with anatomic tomographic imaging methods, the differences were clear: PET detected more foci in the neck (37 patients) and the mediastinum (33 patients) than the others did (Figs. 2 and 3), but PET failed to localize many lesions in the lung and the liver.  $^{131}\text{I}$ -MIBG planar scintigraphy findings were positive for only 3 patients. The results with this method (2 cervical, 1 mediastinal, and 1 bony lesion) did not add any information to that furnished by the other diagnostic examinations. For 2 patients, despite the elevated calcitonin level (patient 22, 40.2 ng/mL; patient 33, 21.5 ng/mL), all the examinations failed to localize any metastases. The results of PET, CT, and MRI were considered to be false-negative for both patients.

Aspiration cytology or surgical intervention assisted in the verification of localized cervical, supraclavicular, and mediastinal lymph node metastases in 10 patients. Although not all PET-detected lesions were proven pathologically, subsequent noninvasive radiologic examinations revealed

**TABLE 1**  
Patient Characteristics

Patient no.	Sex	Age (y)	Year of diagnosis	Initial pathologic stage	Surgery	Other therapy	Type of cancer	Calcitonin (ng/mL) at time of PET	CEA (ng/mL) at time of PET	Flush/diarrhea	Results of PET confirmed by	Follow-up (mo)
1	M	60	1995	pT4 pNX MX	BS ST	RN, irradi	Spor	298.00	9.4	—	—	62
2	F	46	1996	pT3 pN0 MX	NT, BS LND	Irradi	Spor	311.00	112.9	+	—	59
3	M	42	1998	pT3 N1b MX	ST, C LNP	Irradi	Spor	1,070.00	5.2	—	Patho	24
4	F	44	1997	pT4 N1a MX	NT, L LND	Irradi	Spor	3,574.00	31.7	—	Radi	42
5	F	25	1998	pT2 pN1a MX	ST, 2 R LNP	Irradi	MEN 2a	5,827.00	7.9	+	Patho	33
6	M	29	1998	pT2 pN1b MX	TT, BS LND + Sc + C	Irradi	ND	4,209.00	353.0	+	Radi	24
7	F	43	1995	pT2 pN1a M0	NT, BS LND	Irradi	MEN 2a	21.00	0.7	—	—	70
8	M	47	1985	pT3 pN1a M0	R NT	Chemo	ND	1,880.00	399.4	+	Patho	187
9	M	54	1998	pT2 pN1b M0	NT, L LND + C	Irradi	MEN 2b	32.00	2.2	—	—	32
10	F	59	1992	pT3 pNX M0	ST	NP	Spor	826.00	0.5	—	Patho	105
11	F	47	1994	pT1 pNX M0	ST	NP	FMTc	18.70	0.6	—	—	72
12	F	46	1994	pT2 pN1a M0	ST, R LND	RN, irradi	Spor	211.00	401.3	—	Patho	78
13	M	67	1999	pT2 pN1a MX	TT, R LND + Sc	Irradi	Spor	1,627.00	6.5	+	Radi	20
14	F	56	1989	pT2 pNX M0	ST	RN, irradi	FMTc	131.00	5.4	—	Radi	133
15	M	21	1998	pT3 pN1b MX	NT, R LND + Medi	Chemo, irradi	ND	3,954.00	207.3	+	Radi	35
16	F	51	1969	pT3 pN1a M0	ST, L LNP	Irradi	MEN 2a	14.50	8.7	—	—	379
17	F	41	1997	pT4 pNX M0	Sterectomy	Irradi	MEN 2a	1,631.00	157.9	—	Patho	38
18	M	23	1997	pT1 pN1b MX	TT, BS LND	Irradi	MEN 2b	526.00	7.9	—	Patho	40
19	F	60	1983	pT3 pN0 MX	ST, R LND	RN	Spor	1,396.00	22.9	—	Radi	208
20	M	58	1998	pT2 pN1a MX	NT, R LND	Irradi	Spor	91.00	14.7	—	Radi	33
21	M	40	1993	pT1 pN1a MX	NT, L LND	RN, irradi	ND	521.00	3.3	—	Radi	92
22	F	41	1998	pT2 pNX MX	NT	NP	Spor	40.20	0.5	—	—	33
23	F	69	1992	pT2 pN1a M0	NT, R LND	RN, irradi	Spor	999.00	6.9	—	—	97
24	M	38	1990	pT2 pN1a MX	TT, L LND	Irradi	ND	240.00	7.4	—	Patho	128
25	F	49	1997	pT2 pNX MX	NT	Irradi	Spor	379.00	5.7	—	Radi	41
26	F	62	1979	pT3 pN1a MX	NT, L LND	Chemo, irradi	Spor	2,500.00	105.0	—	Radi	255
27	M	52	1999	pT3 pNX MX	NT	NP	FMTc	2,844.00	694.5	+	Patho	21
28	M	48	1999	pT2 pN0 M0	TT, BS LND	NP	MEN 2a	24.00	1.9	—	—	20
29	M	46	1994	pT2 pNX M0	ST, L LND	Irradi	FMTc	2,213.00	11.4	—	Patho	58 (death)
30	M	34	1994	pT2 pN1b MX	ST, L LND + Sc + C	RN, irradi	MEN 2a	584.00	37.9	—	Radi	72
31	F	50	1990	pT3 pNX MX	TT, Medi	Irradi	ND	3,974.00	31.9	—	Radi	127
32	F	55	1990	pT2 pNX MX	NT	NP	Spor	56.00	0.1	+	Radi	129
33	F	45	1999	pT1 pN0 M0	ST, L LNP	NP	Spor	21.50	1.2	—	—	17
34	F	54	1984	pT3 pN1a M0	NT, L LND	Irradi	Spor	326.00	5.7	—	Radi	199
35	F	66	1997	pT3 pN0 M0	TT, BS LND	Irradi	MEN 2a	279.00	2.3	—	—	38
36	M	48	1997	pT4 pN1b MX	NT, R LND + Sc + C	Irradi	Spor	3,496.00	277.1	—	—	46
37	M	66	1997	pT2 pN1b MX	NT, R LND + C	Irradi	Spor	2,692.00	54.4	—	Radi	36
38	F	51	1998	pT2 pNX M0	TT	NP	Spor	90.80	3.3	+	—	31
39	F	68	1994	pT3 pN1b M0	ST, C LNP	Irradi	MEN 2a	39.00	11.9	—	—	78
40	M	35	1997	pT4 pN1b MX	NT, BS LND + C	Irradi	MEN 2a	891.00	23.5	—	—	38

BS = both sides; ST = subtotal thyroidectomy; RN = radionuclide ( $^{131}\text{I}$ -MIBG) therapy; irradi = external irradiation; spor = sporadic; NT = near total thyroidectomy; LND = lymph node dissection; C = central; LNP = lymph node picking; patho = histology/cytology; radi = radiology; MEN 2a = multiple endocrine neoplasia type 2a; TT = total thyroidectomy; Sc = supraclavicular; ND = not determined; chemo = chemotherapy; MEN 2b = multiple endocrine neoplasia type 2b; NP = not performed; FMTc = familial MTC; medi = mediastinal.

**TABLE 2**  
Number of Patients with Detected Manifestations

Site	PET	CT	MRI	<sup>131</sup> I-MIBG
Lymph node	38	26	19	3
Liver	7	9	6	0
Lung	2	5	2	0
Bone	5	0	1	1
Breast	1	1	1	0
Total*	38	29	23	3
Scanning not performed	0	0	5	0

\*Total number of scans with positive findings.

pathologic lymph node enlargement or hepatic, pulmonary, or bone metastases in 15 patients. Small hepatic metastases were detected in 35 patients who underwent hepatic angiography. PET imaging revealed 2 cases of suspected bony metastases. In the case of the solitary metastasis, tumorous manifestation was supported by CT, MRI, and somatostatin receptor scintigraphy, but 2 completed biopsies (each reported by 2 independent pathologists) excluded the presence of metastatic disease. The other case also proved to be false-positive on the basis of the 3-y uneventful follow-up. Although the above methods supported the PET findings in a substantial proportion of our patients, the data on some patients still require validation. However, these patients have shown no clinical signs contradicting the PET findings.

The data obtained during the follow-up from the initial diagnosis (Table 1) clearly show the relatively benign clinical course of MTC: Only 1 patient has died during a mean follow-up of 81 mo (range, 17–379 mo) in the group with a definitive sign (hypercalcitoninemia) of metastatic disease.

## DISCUSSION

Postoperative elevated or rising calcitonin and CEA levels often prompt the search for residual or recurrent MTC tissue. Conventional imaging methods (CT, MRI, and <sup>131</sup>I-MIBG scintigraphy) frequently fail to reveal these tumorous lesions, because each modality has its own limitations.

In this study, we compared the findings of conventional diagnostic imaging with those of <sup>18</sup>F-FDG PET in the in-



**FIGURE 1.** Sagittal slice shows high <sup>18</sup>F-FDG accumulation in right breast of patient 17.

vestigation and restaging of MTC. Although CT and MRI detected a higher percentage of pulmonary and hepatic metastases than did <sup>18</sup>F-FDG PET, <sup>18</sup>F-FDG PET was superior in detecting lymph node involvement. We succeeded in identifying metastatic lymph nodes in all but 2 investigated MTC patients with elevated plasma tumor marker levels, and the number of detected lesions was higher than that found with any of the other conventional methods. In addition, the lack of attenuation correction probably decreased the tumor detection rate of PET, especially for the smaller tumors.

Lymph nodes in the cervical and mediastinal regions represent the first lymphatic levels of thyroid cancer. The lower number of involved cervical lymph nodes is explained by the fact that cervical dissections had been performed previously in many cases. Nevertheless, the number

**TABLE 3**  
Number of Affected Lymphatic Regions (Nodes) Detected

Imaging technique	Cervical			Supraclavicular		Axillary		Mediastinal	Abdominal
	Left	Right	Central	Left	Right	Left	Right		
CT	9 (15)	9 (11)	6 (8)	3 (5)	1 (1)	2 (2)	1 (1)	14 (39)	1 (3)
MRI	8 (13)	8 (10)	8 (11)	1 (2)	2 (3)	0 (0)	1 (1)	11 (35)	0 (0)
PET	22 (35)	19 (33)	21 (30)	8 (14)	8 (11)	2 (3)	1 (1)	33 (117)	2 (3)

Numbers of lymph nodes positive for cancer are given in parentheses.



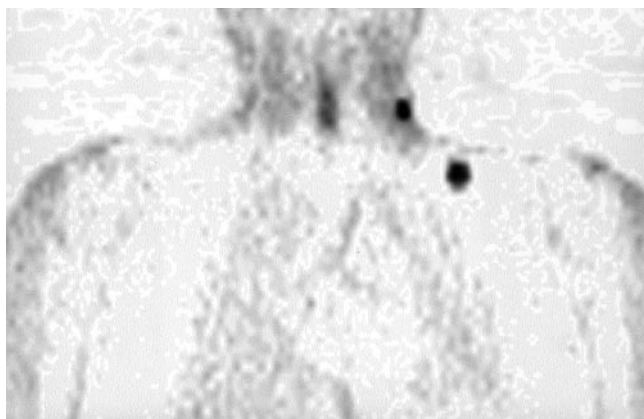


**FIGURE 2.**  $^{18}\text{F}$ -FDG PET shows high tracer uptake in left lateral cervical compartment and in left supraclavicular region of patient 24. Radiologic methods detected lymph node only in left supraclavicular region. Histology confirmed metastases of MTC in both sites.

of involved cervical lymph nodes identified postsurgically seems surprisingly high, indicating the predominantly incomplete nature of the cervical dissections in the investigated group. This strategy is far from optimal. Prevalently systematic (cervical and mediastinal) lymph node dissection would help to avoid the early serious consequences (e.g., compression symptoms) of centrally located lymph node metastases. Our results indicate that MTC patients with an elevated calcitonin level during the follow-up display foci with a high tracer accumulation in at least one of the lymphatic regions (38/40 [95%]). This finding is in keeping with a reported lymph node metastasis incidence of 94% in hypercalcitoninemic patients after primary therapy (36).

In our study, small pulmonary metastases (<1 cm) detected by CT (and MRI) were not visualized by  $^{18}\text{F}$ -FDG PET. Data in the literature indicate a low sensitivity of  $^{18}\text{F}$ -FDG PET for small pulmonary metastases (27,29). A helical CT scan of the lung is therefore recommended if pulmonary metastasis is suspected.

Although this study detected metastases in all but 2 patients, a mismatch between the serum calcitonin level and the detected mass was found in many cases. The probable explanation for this mismatch was addressed by Ésik et al. (37), who reported a near-total prevalence of small hyper-



**FIGURE 3.** Coronal slices show multiple  $^{18}\text{F}$ -FDG accumulation in mediastinum and both pulmonary hila of patient 36.

vascular hepatic metastases in these cases. Our follow-up data (35 patients with angiographically proven hepatic metastases, of whom only 7 had positive PET findings for the liver) support this observation.

With  $^{131}\text{I}$ -MIBG scintigraphy, only 3 of the 40 patients investigated had positive scan findings. The limited uptake of this tracer indicates the poor and questionable diagnostic value of this method for the detection of recurrent MTC.

The results of this study lead us to recommend  $^{18}\text{F}$ -FDG PET examinations of MTC patients with postoperative elevated plasma tumor marker levels to select patients for secondary surgical intervention. If many lymph nodes are involved, a conservative approach (e.g., external irradiation) may be chosen as the appropriate treatment (38). Meticulous dissection is recommended in cases of limited dissemination or if some of the lymph node localizations are unfavorable (39). These centrally located metastatic lymph nodes in the neck and upper mediastinum represent metastases that may seriously affect the quality of life (39,40).

## CONCLUSION

Our results indicate that  $^{18}\text{F}$ -FDG PET investigation is a highly sensitive method for the detection of metastases in MTC patients with elevated tumor marker levels. Its sensitivity surpasses that of other imaging procedures, especially in the localization of cervical and mediastinal lymph node involvement.

## ACKNOWLEDGMENTS

This study was supported in part by grant 219/2000 from the Scientific Health Care Council and grant T-29809 from the National Scientific Research Fund.

## REFERENCES

1. Marsh DJ, Learoyd DL, Robinson BG. Medullary thyroid carcinoma: recent advances and management update. *Thyroid*. 1995;5:407–424.
2. Dralle H, Damm I, Scheumann GF, Kotzerke J, Kupsch E. Frequency and significance of cervicomediastinal lymph node metastases in medullary thyroid carcinoma: results of a compartment-oriented microdissection method. *Henry Ford Hosp Med J*. 1992;40:264–267.
3. Schröder S, Böcker W, Baisch H, et al. Prognostic factors in medullary thyroid carcinomas: survival in relation to age, sex, stage, histology, immunocytochemistry, and DNA content. *Cancer*. 1988;61:806–816.
4. Simpson WJ, Palmer JA, Rosen IB, Mustard RA. Management of medullary carcinoma of the thyroid. *Am J Surg*. 1982;144:420–422.
5. Bergholm U, Adami HO, Bergstrom R, et al. Clinical characteristics in sporadic and familial medullary thyroid carcinoma: a nationwide study of 249 patients in Sweden from 1959 through 1981. *Cancer*. 1989;63:1196–1204.
6. DeLellis RA, Rule AH, Spiler I, Nathanson L, Tashjian AH Jr, Wolfe HJ. Calcitonin and carcinoembryonic antigen as tumour markers in medullary thyroid carcinoma. *Am J Clin Pathol*. 1978;70:587–594.
7. Norton JA, Doppman JL, Brennan MF. Localization and resection of clinically inapparent medullary carcinoma of the thyroid. *Surgery*. 1980;87:616–622.
8. Abdelmoumene N, Schlumberger M, Gardet P, et al. Selective venous sampling catheterisation for localisation of persisting medullary thyroid carcinoma. *Br J Cancer*. 1994;69:1141–1144.
9. Schwerk WB, Grün R, Wahl R. Ultrasound diagnosis of C-cell carcinoma of the thyroid. *Cancer*. 1985;55:624–630.
10. Crow JP, Azar-Kia B, Prinz RA. Recurrent occult thyroid carcinoma detected by MR imaging. *AJR*. 1989;152:1255–1256.
11. Frank-Raue K, Raue F, Buhr HJ, Baldauf G, Lorenz D, Ziegler R. Localization of occult persisting medullary thyroid carcinoma before microsurgical reopera-

- tion: high sensitivity of selective venous catheterization. *Thyroid*. 1992;2:113–117.
12. Raue F, Winter J, Frank-Raue K, Lorenz D, Herfarth C, Ziegler R. Diagnostic procedure before reoperation in patients with medullary thyroid carcinoma. *Horm Metab Res Suppl*. 1989;21:31–34.
  13. Dörr U, Würstlin S, Frank-Raue K, et al. Somatostatin receptor scintigraphy and magnetic resonance imaging in recurrent medullary thyroid carcinoma: a comparative study. *Horm Metab Res Suppl*. 1993;27:48–55.
  14. Wang Q, Takashima S, Fukuda H, Takayama F, Kobayashi S, Sone S. Detection of medullary thyroid carcinoma and regional lymph node metastases by magnetic resonance imaging. *Arch Otolaryngol Head Neck Surg*. 1999;125:842–848.
  15. Hoefnagel CA, Delprat CC, Zanin D, van der Schoot JB. New radionuclide tracers for the diagnosis and therapy of the medullary thyroid carcinoma. *Clin Nucl Med*. 1988;13:159–165.
  16. Baudin E, Lumbroso J, Schlumberger M, et al. Comparison of octreotide scintigraphy and conventional imaging in medullary thyroid carcinoma. *J Nucl Med*. 1996;37:912–916.
  17. Learoyd DL, Roach PJ, Briggs GM, Delbridge LW, Wilmshurst EG, Robinson BG. Technetium-99-sestamibi scanning in recurrent medullary thyroid carcinoma. *J Nucl Med*. 1997;38:227–230.
  18. Manil L, Boudet F, Motte P, et al. Positive anticalcitonin immunoscintigraphy in patients with medullary thyroid carcinoma. *Cancer Res*. 1989;49:5480–5485.
  19. Peltier P, Curtet C, Chatal J-F, et al. Radioimmunodetection of medullary thyroid cancer using a bispecific anti-CEA/anti-indium-DTPA antibody and an indium-111-labeled DTPA dimer. *J Nucl Med*. 1993;34:1267–1273.
  20. Troncone L, Rufini V, Montemaggi P, Danza FM, Lasorella A, Mastrangelo R. The diagnostic and therapeutic utility of radioiodinated metaiodobenzylguanidine (MIBG): 5 years of experience. *Eur J Nucl Med*. 1990;16:325–335.
  21. Ugur Ö, Kostakoglu L, Güler N, et al. Comparison of  $^{99m}\text{Tc}(\text{V})\text{-DMSA}$ ,  $^{201}\text{Tl}$  and  $^{99m}\text{Tc}\text{-MIBI}$  imaging in the follow-up of patients with medullary carcinoma of the thyroid. *Eur J Nucl Med*. 1996;23:1367–1371.
  22. Berna L, Chico A, Matias-Guiu X, et al. Use of somatostatin analogue scintigraphy in the localization of recurrent medullary thyroid carcinoma. *Eur J Nucl Med*. 1998;25:1482–1488.
  23. Strauss LG, Conti PS. The application of PET in clinical oncology. *J Nucl Med*. 1991;32:623–648.
  24. Joensuu H, Ahonen A. Imaging of metastases of thyroid carcinoma with fluorine-18-fluorodeoxyglucose. *J Nucl Med*. 1987;28:910–914.
  25. Grünwald F, Källicke T, Feine U, et al. Fluorine-18 fluorodeoxyglucose positron emission tomography in thyroid cancer: results of a multicenter study. *Eur J Nucl Med*. 1999;26:1547–1552.
  26. Sisson JC, Ackermann RJ, Meyer MA, Wahl RL. Uptake of 18-fluoro-2-deoxy-D-glucose by thyroid cancer: implications for diagnosis and therapy. *J Clin Endocrinol Metab*. 1993;77:1090–1094.
  27. Grünwald F, Schomburg A, Bender H, et al. Fluorine-18 fluorodeoxyglucose positron emission tomography in the follow-up of differentiated thyroid cancer. *Eur J Nucl Med*. 1996;23:312–319.
  28. Feine U, Lietzenmayer R, Hanke J-P, Held J, Wöhrle H, Müller-Schauenburg W. Fluorine-18-FDG and iodine-131-iodide uptake in thyroid cancer. *J Nucl Med*. 1996;37:1468–1472.
  29. Dietlein M, Scheidhauer K, Voth E, Theissen P, Schicha H. Fluorine-18 fluorodeoxyglucose positron emission tomography and iodine-131 whole-body scintigraphy in the follow-up of differentiated thyroid cancer. *Eur J Nucl Med*. 1997;24:1342–1348.
  30. Scott GC, Meier DA, Dickinson CZ. Cervical lymph node metastasis of thyroid papillary carcinoma imaged with fluorine-18-FDG, technetium-99m-per technetate and iodine-131-sodium iodide. *J Nucl Med*. 1995;36:1843–1845.
  31. Conti PS, Durski JM, Bacqai F, Grafton ST, Singer PA. Imaging of locally recurrent and metastatic thyroid cancer with positron emission tomography. *Thyroid*. 1999;9:797–804.
  32. Adams S, Baum R, Rink T, Schumm-Dräger PM, Usadel KH, Hör G. Limited value of fluorine-18 fluorodeoxyglucose positron emission tomography for the imaging of neuroendocrine tumours. *Eur J Nucl Med*. 1998;25:79–83.
  33. Musholt TJ, Musholt PB, Dehdashti F, Moley JF. Evaluation of fluorodeoxyglucose-positron emission tomographic scanning and its association with glucose transporter expression in medullary thyroid carcinoma and pheochromocytoma: a clinical and molecular study. *Surgery*. 1997;122:1049–1060.
  34. Gasparoni P, Rubello D, Ferlin G. Potential role of fluorine-18-deoxyglucose (FDG) positron emission tomography (PET) in the staging of primitive and recurrent medullary thyroid carcinoma. *J Endocrinol Invest*. 1997;20:527–530.
  35. Brand-Mainz K, Müller SP, Görges R, Saller B, Bockisch A. The value of fluorine-18 fluorodeoxyglucose PET in patients with medullary thyroid cancer. *Eur J Nucl Med*. 2000;27:490–496.
  36. Gimm O, Dralle H. Reoperation in metastasizing medullary thyroid carcinoma: is a tumour stage-oriented approach justified? *Surgery*. 1997;122:1124–1130.
  37. Ésik O, Szavcsur P, Szakáll S Jr, et al. Angiography effectively supports the diagnosis of hepatic metastases in medullary thyroid carcinoma. *Cancer*. 2001;91:2084–2095.
  38. Vitale G, Caraglia M, Ciccirelli A, et al. Current approaches and perspectives in the therapy of medullary thyroid carcinoma. *Cancer*. 2001;91:1797–1808.
  39. Chen H, Roberts JR, Ball DW, et al. Effective long-term palliation of symptomatic, incurable metastatic medullary thyroid cancer by operative resection. *Ann Surg*. 1998;227:887–895.
  40. Machens A, Gimm O, Ukkat J, Hinze R, Schneyer U, Dralle H. Improved prediction of calcitonin normalization in medullary thyroid carcinoma patients by quantitative lymph node analysis. *Cancer*. 2000;88:1909–1915.





The Journal of  
NUCLEAR MEDICINE

## **$^{18}\text{F}$ -FDG PET Detection of Lymph Node Metastases in Medullary Thyroid Carcinoma**

Szabolcs Szakáll, Jr., Olga Ésik, Gábor Bajzik, Imre Repa, Gabriella Dabasi, István Sinkovics, Péter Ágoston and Lajos Trón

*J Nucl Med.* 2002;43:66-71.

---

This article and updated information are available at:  
<http://jnm.snmjournals.org/content/43/1/66>


---

Information about reproducing figures, tables, or other portions of this article can be found online at:  
<http://jnm.snmjournals.org/site/misc/permission.xhtml>

Information about subscriptions to JNM can be found at:  
<http://jnm.snmjournals.org/site/subscriptions/online.xhtml>

*The Journal of Nuclear Medicine* is published monthly.  
SNMMI | Society of Nuclear Medicine and Molecular Imaging  
1850 Samuel Morse Drive, Reston, VA 20190.  
(Print ISSN: 0161-5505, Online ISSN: 2159-662X)

© Copyright 2002 SNMMI; all rights reserved.

 SOCIETY OF  
NUCLEAR MEDICINE  
AND MOLECULAR IMAGING